Electron Photodetachment of Cyclopentadienylidene Anion Radical in a Flowing Afterglow Apparatus: EA and $\Delta H_f°$ of Cyclopentadienylidene

Richard N. McDonald,* Edward J. Bianchina Jr., and Cheng C. Tung

Contribution from the Department of Chemistry, Kansas State University, Manhattan, Kansas 66502. *Received December 3, 1990*

Abstract: The thresholds for electron photodetachment (EPD) from the doublet ground electronic state of cyclopentadienylidene anion radical (c-$C_5H_4^{\bullet-}$) producing the $^3B_1$ ground state of cyclopentadienylidene, and the $^1A_2$, $^3A_2$, and $^1A'$ (latter tentative) excited states of the carbene, have been measured. The assignments of the observed transitions to the excited states of the carbene are based on the good agreement between the measured and theoretical energy gaps for the ground and excited states for this system. The EPD thresholds occur at 708 (40.4 ± 1.08 kcal mol^{-1}), 619 (46.2 ± 0.23 kcal mol^{-1}), 598 (47.8 ± 0.23 kcal mol^{-1}), and 576 nm (49.6 ± 0.23 kcal mol^{-1}), respectively. From the previously determined $\Delta H°_{f,298}$(c-$C_5H_4^{\bullet-}$) = 71.9 ± 3.6 kcal mol^{-1}, $\Delta H°_{f,298}$($^3B_1$ c-C_5H_4) = 112.3 ± 4.7 kcal mol^{-1} is determined. The $\Delta H_f°$ of the observed excited states of the carbene are also given.

Introduction

The determination of electron affinities (EA) of atomic and molecular species[1] is important to a number of disciplines ranging from gas-phase negative ion chemistry to charge transfer in inorganic, organic, and catalytic condensed-phase reactions and to electron transfer in biological systems. To measure this important thermodynamic property, a variety of methods have been used; in a review by Christodoulides et al.,[1a] 31 methods are discussed. Several of these methods involve photodetachment of the negative ion (eq 1) and are generally agreed to yield the most accurate

$$A^- + h\nu \rightarrow A + e^- \quad (1)$$

EA data.[2] These photon impact methods include photoelectron spectroscopy (PES) and electron photodetachment (EPD). In PES experiments, the output of a fixed-frequency laser crosses the ion beam and the kinetic energy of the detached electrons is measured. The difference in the incident photon and detached electron energies for the 0–0 transition (following certain corrections) is the EA of neutral A.[2b]

In EPD experiments, a tunable light source is employed. The negative ion generation methods for EPD measurements include high-pressure drift tubes,[3,4] ion cyclotron resonance (ICR) spectrometers,[5-8] and crossed-beam[9,10] and coaxial ion-laser beam apparatus.[11-13] EPD cross section vs wavelength plots are generated from the loss of a percentage of the negative ion signal as a function of photon energy by using conventional or laser photon sources. The EPD threshold is then determined. In favorable cases, the 0–0 transition is observed yielding the EA(A), and vibrational and excited electronic state spacings in A^- and A can be obtained.

In general, the lowest energy required to achieve photodetachment will yield an accurate threshold. The Franck–Condon factors strongly influence the photodetachment behavior of A^- near threshold. A problem arises with polyatomic molecules if the structures of the ion and the corresponding neutral differ significantly. This results in poor Franck–Condon overlap, and the detachment threshold may involve transitions from the ground state of the anion to upper vibrational levels of the neutral, and overestimates the EA(A). Further, transitions from higher vibrational states of the anion to the neutral ground state (hot bands) will underestimate EA(A) unless properly identified. However, such errors are likely to be <0.1 eV.

In our gas-phase studies of the generation, thermodynamic properties, and chemistry of carbene anion radicals ($R_2C^{\bullet-}$), a flowing afterglow (FA) apparatus was used.[14] In all cases, the $\Delta H°_{f,298}(R_2C^{\bullet-})$ were determined. If we could effect EPD with $R_2C^{\bullet-}$ (+ $h\nu \rightarrow R_2C + e^-$) to measure EA($R_2C$), the $\Delta H°_{f,T}(R_2C)$ would be experimentally determined by eq 2 for a number of

$$\Delta H°_{f,T}(R_2C) = \Delta H°_{f,T}(R_2C^{\bullet-}) + EA(R_2C) \quad (2)$$

polyatomic carbenes. Since $\Delta H°_{f,T}(R_2C^{\bullet-})$ is a 298 K value and EA(R_2C) is a threshold 0 K value, conventional corrections from T = 298 to 0 K can be made if desired. If the geometries of $R_2C^{\bullet-}$ and R_2C are not appreciably different, the EA(R_2C) at 298 K can be approximated by the 0 K value. The necessary flange-mounts for optical windows were added to the FA. The overall EPD equipment design follows closely that described by Moseley et al.,[15] who used a drift tube in their experiments. We report here the results of our first studies with this apparatus that include two test cases (EPD of acetophenone enolate and cyclopentadienyl anions) and the target of this investigation, the EPD of cyclopentadienylidene anion radical (c-$C_5H_4^{\bullet-}$).

(1) (a) Christodoulides, A. A.; McCorkle, D. L.; Christophorou, L. G. In *Electron-Molecule Interactions and Their Applications*; Christophorou, L. G., Ed.; Academic Press: New York, 1984; Vol. 2, Chapter 6. (b) For a recent review of additional EAs, see Kebarle, P.; Chowdhury, S. *Chem. Rev.* **1987**, *87*, 513.

(2) (a) Miller, T. M. *Adv. Electron. Electron Phys.* **1981**, *55*, 119. (b) Mead, R. D.; Stevens, A. E.; Lineberger, W. C. In *Gas Phase Ion Chemistry*; Bowers, M. T., Ed.; Academic Press: New York, 1984; Vol. 3, Chapter 22.

(3) Woo, S. B.; Helmy, E. M.; Mauk, P. H.; Paszek, A. P. *Phys. Rev.* **1981**, *64*, 1380.

(4) Moseley, J. T. In *Applied Atomic Collision Physics*; Massey, H. S. W., McDaniel, E. W., Bederson, B., Eds.; Academic Press: New York, 1982; Vol. 5, p 269.

(5) Janousek, B. K.; Brauman, J. I. In *Gas Phase Ion Chemistry*; Bowers, M. T., Ed.; Academic Press: New York, 1979; Vol. 2, Chapter 10.

(6) Blumberg, W. A. M.; Itano, W. M.; Larson, D. J. *Phys. Rev. D* **1979**, *19*, 139.

(7) Drzaic, P. S.; Marks, J.; Brauman, J. I. In *Gas Phase Ion Chemistry*; Bowers, M. T., Ed.; Academic Press: New York, 1984; Vol. 3, Chapter 21.

(8) Wetzel, D. M.; Brauman, J. I. *Chem. Rev.* **1987**, *87*, 607.

(9) Slater, J.; Read, F. H.; Novick, S. E.; Lineberger, W. C. *Phys. Rev. A* **1978**, *17*, 201.

(10) Jones, P. L.; Mead, R. D.; Kohler, B. E.; Rosner, S. D.; Lineberger, W. C. *J. Chem. Phys.* **1980**, *78*, 4419.

(11) Moseley, J. T.; Durup, J. *Annu. Rev. Phys. Chem.* **1981**, *32*, 53.

(12) Hefter, U.; Mead, R. D.; Schulz, P. A.; Lineberger, W. C. *Phys. Rev. A* **1983**, *28*, 1429.

(13) Carrington, A.; Kennedy, R. A. In *Gas Phase Ion Chemistry*; Bowers, M. T., Ed.; Academic Press: New York, 1984; Vol. 3, Chapter 26.

(14) For a recent review of this subject, see: McDonald, R. N. *Tetrahedron* **1989**, *45*, 3993.

(15) (a) Moseley, J. T.; Cosby, P. C.; Bennett, R. A.; and Peterson, J. R. *J. Chem. Phys.* **1975**, *62*, 4826. (b) Cosby, P. C.; Bennett, R. A.; Peterson, J. R.; Moseley, J. T. *Ibid.* **1975**, *63*, 1612. (c) Moseley, J. T.; Cosby, P. C.; Peterson, J. R. *Ibid.* **1976**, *65*, 2512. (d) Cosby, P. C.; Ling, J. H.; Peterson, J. R.; Moseley, J. T. *Ibid.* **1976**, *65*, 5267. (e) Huber, B. A.; Cosby, P. C.; Peterson, J. R.; Moseley, J. T. *Ibid.* **1977**, *66*, 4520. (f) Smith, G. P.; Cosby, P. C.; Moseley, J. T. *Ibid.* **1977**, *67*, 3818. (g) Smith, G. P.; Lee, L. C.; Cosby, P. C.; Peterson, J. R.; Moseley, J. T. *Ibid.* **1978**, *68*, 3818. (h) Cosby, P. C.; Moseley, J. T.; Peterson, J. R.; Ling, J. H. *Ibid.* **1978**, *69*, 2771. (i) Cosby, P. C.; Smith, G. P.; Moseley, J. T. *Ibid.* **1978**, *69*, 2779. (j) Lee, L. C.; Smith, G. P.; Moseley, J. T.; Cosby, P. C.; Guest, J. A. *Ibid.* **1979**, *70*, 3237. (k) Smith, G. P.; Lee, L. C.; Moseley, J. T. *Ibid.* **1979**, *71*, 4034. (l) Hodges, R. V.; Lee, L. C.; Moseley, J. T. *Ibid.* **1980**, *72*, 2998.

0002-7863/91/1513-7115$02.50/0

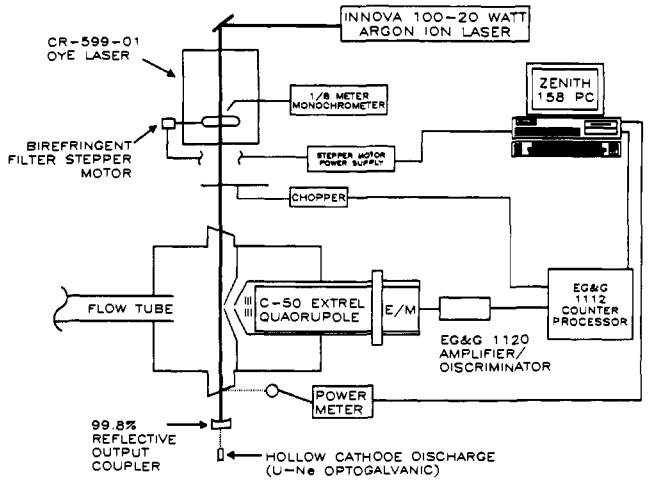

Figure 1. Schematic diagram of the FA and the associated equipment for the EPD experiments.

Experimental Section

The FA used to generate the negative ions in these studies has been described.[16] The three negative ions, acetophenone enolate anion ($C_6H_5C(O^-)=CH_2$), cyclopentadienyl anion (c-$C_5H_5^-$), and cyclopentadienylidene anion radical (c-$C_5H_4^{\bullet-}$), were produced according to eqs 3–5. In reactions 3 and 4, the F^- and CH_3O^- ions were generated

$$C_6H_5C(=O)CH_3 + F^- \rightarrow \underset{m/z\ 119}{C_6H_5C(O^-)=CH_2} + HF \quad (3)$$

$$c\text{-}C_5H_6 + CH_3O^- \rightarrow \underset{m/z\ 65}{c\text{-}C_5H_5^-} + HOCH_3 \quad (4a)$$

$$\text{or } c\text{-}C_5H_6 + F^- \rightarrow c\text{-}C_5H_5^- + HF \quad (4b)$$

$$c\text{-}C_5H_4{=}N_2 + e^- \rightarrow \underset{m/z\ 64}{c\text{-}C_5H_4^{\bullet-}} + N_2 \quad (5)$$

by dissociative electron attachment with NF_3 and CH_3ONO, respectively. These organic negative ions were formed in the upstream end of the flow tube in a region ca. 120–135 cm from the first ion-sampling nose cone orifice. The absence of free electrons downstream of this ion-generation region was determined by the addition of SF_6. If the signal for $SF_6^{\bullet-}$ was detected, the flow of the neutral substrate was increased until the $SF_6^{\bullet-}$ ion signal was absent at high sensitivity of the electron multiplier.

The organic negative ions undergo numerous collisions with the helium buffer gas as they traverse the length of the flow tube (typical flow parameters were $P_{He} = 0.8$ Torr and $\bar{v} = 50$ m s^{-1}). Under these conditions, the ions are collisionally cooled to 298 K, and their average residence time in the 2-mm photon beam (ca. 0.04 ms) is determined by the helium bulk flow velocity.

For the EPD experiments, the quadrupole mass filter (Extrel C-50, 10–1200-amu range) was operated in the single-ion mode with the rf and dc potentials on the rods set to pass only those negative ions of interest (m/z 119, 65, or 64). Typically, the mass resolution of the mass filter was set so that the base of the "single" ion peak covered 2–5 amu. This allowed for increased ion counts and improved signal-to-noise ratios.

The schematic diagram for the FA, the lasers, and the associated equipment for the EPD experiments is shown in Figure 1. The laser system consists of a Coherent tunable dye laser (CR-599-01) pumped by the all-line visible output of a Coherent argon ion laser (Innova 100-20). Because of the short interaction time of the negative ions with the photons, we require the high photon flux inside the cavity of the dye laser for the EPD experiments to improve the electron photodetachment probability. The cavity of the dye laser was extended to include the FA by replacing the standard, flat output coupler (ca. 95% reflective) of the dye laser with a more highly reflective concave mirror (CVI Laser Corp., maximum >99.8% reflective, 1.5-m radius of curvature[17]) and placing the mirror on the far side of the FA. With eliptical fused silica windows (2.5-cm minor diameter, 3 mm thick) epoxided on flanges at Brewsters angle on the front and rear plates of the FA, the FA is now inside the extended cavity of the dye laser.[18,19]

The alignment of the laser beam in the extended cavity experiments is critical. The ~2-mm diameter photon beam passes just in front of the 1-mm orifice of the first ion-sampling molybdenum nose cone in the FA. Final alignment was done with the ion flow established to obtain the maximum percentage of EPD at the wavelength with the highest laser intensity of the dye in use.

The chopper (EG&G Model 196) modulated the photon beam at 100 Hz to give laser-on and laser-off cycles. The chopper control sent trigger signals to the EG&G photon counter/processor (Model 1112) to correctly direct the separate ion counts for the laser-on and laser-off half-cycles to the two counters in the EG&G Model 1112. The sampling interval for these half-cycles is adjusted to avoid possible edge effects of the chopper square wave. The EG&G amplifier/discriminator (Model 1120), which had been adjusted for the correct count threshold level, converted the anlogue signal from the channeltron multiplier of the mass spectrometer to a digital TTL pulse signal for input to the photon counter/processor.

The photon counter/processor handles eight digits of ion counts in its data registers, but only outputs the first three digits and an exponent following preset arithmetic processing for display and to its output buffers. A homemade circuit was made to recover all eight digits of the data for the laser-on and laser-off cycles and transfer them directly to the computer when a preset value of chopper cycles was achieved. In the normal experimental condition, the ion counts were accumulated in 0.35 s for each on/off cycle 10 times and the average of these 10 points were used to calculate σ_{rel} for each wavelength.

The circulating power within the extended laser cavity was monitored with a Laser Precision Corp. power meter (Model RT-20) using a reflection from the rear Brewster window of the FA. The intracavity power was calculated from the measured transmission of the output mirror at several fixed wavelengths. The percent reflection from the rear Brewster window (0.1%) was then determined from the ratio of the reflected power and the intracavity power. Typical intracavity powers of 15–50 W were used in these EPD experiments.

When sufficient data at a particular wavelength had been acquired, the computer activated an Oriel stepper motor (Model 17992) to rotate the three-plate birefringent filter to give the next programmed wavelength and data acquisition began again. This was continued until all useable wavelengths of the dye had been examined; usually, data points were taken every 2–3 Å. The starting and final wavelengths (±0.5 nm) of the run were measured with an Oriel $^1/_8$-m monochromator (Model 77250) using a Hamamatsu photodiode detector[20] and adds an uncertainty of ±1 nm to the determinations.

The primary quantity measured in these experiments is the relative cross section for photodestruction of the parent negative ions with photons of specific energies. Since ≥50% of the photodetached electrons can be captured by SF_6 present in the flow and no daughter ions are observed in these photon/ion interactions, these cross sections are the *relative cross sections for EPD*, σ_{rel}. The σ_{rel} are given by the expression in eq 6 where

$$\sigma_{rel}(\lambda) = \frac{\ln (I_0/I)}{\Phi(\lambda)kt} \quad (6)$$

I and I_0 are the average ion counts detected at a given λ for the laser-on and laser-off periods, respectively, and $\Phi(\lambda)$ is the photon flux at that λ.[15a,21] $\Phi(\lambda)$ (photons s^{-1} unit area^{-1}) effectively normalizes the percent EPD to a unit Φ for the different photon fluxs present at the different wavelengths of the dyes employed. The varying intracavity power curves for the dyes used in each experiment are shown as inserts in the σ_{rel} vs λ plots in the Results and Discussion. The additional parameters t, the average time for an ion to traverse the photon beam, and k, the geometric

(16) (a) McDonald, R. N.; Chowdhury, A. K. *J. Am. Chem. Soc.* **1985**, *107*, 4123. (b) McDonald, R. N.; Chowdhury, A. K.; Setser, D. W. *J. Am. Chem. Soc.* **1980**, *102*, 6491.

(17) Each of these mirrors covers a λ range of ca. 700 Å before its transmission exceeds 1% and its utility in these experiments is lost. Their reflectance curves overlap by ca. 80 Å on both ends with other mirrors in the set. In this way, the mirror in use can be replaced by another mirror to complete the spectral range of wavelengths available for each dye.

(18) The two lasers, the chopper, and the monochromator are located on a 4 ft × 8 ft Newport optical table. The mount (Newport Model 600A2) for the highly reflective mirror is bolted to a 4 in. × 6 in. × 3 in. aluminum block and supported on four 8-in.-thick cinder building blocks separated by high-density rubber pads (0.25 in. thick). This arrangement produces no apparent jitter of the extended cavity of the dye laser.

(19) Maguire, T. C.; Brooks, P. R.; Curl, R. F.; Spence, J. H.; Ulvick, S. J. *J. Chem. Phys.* **1986**, *85*, 844.

(20) The wavelength calibration of the monochromator was checked by using six lines (365–811 nm) from an Ar/Kr pen lamp and against a 3-m monochromator.

(21) The use of σ_{rel} assumes constancy of (i) the average time the ion spends crossing the photon beam and (ii) the geometric constant describing the overlap between the photons and that portion of the ion swarm subtended by the detection system. These terms are difficult to determine absolutely.

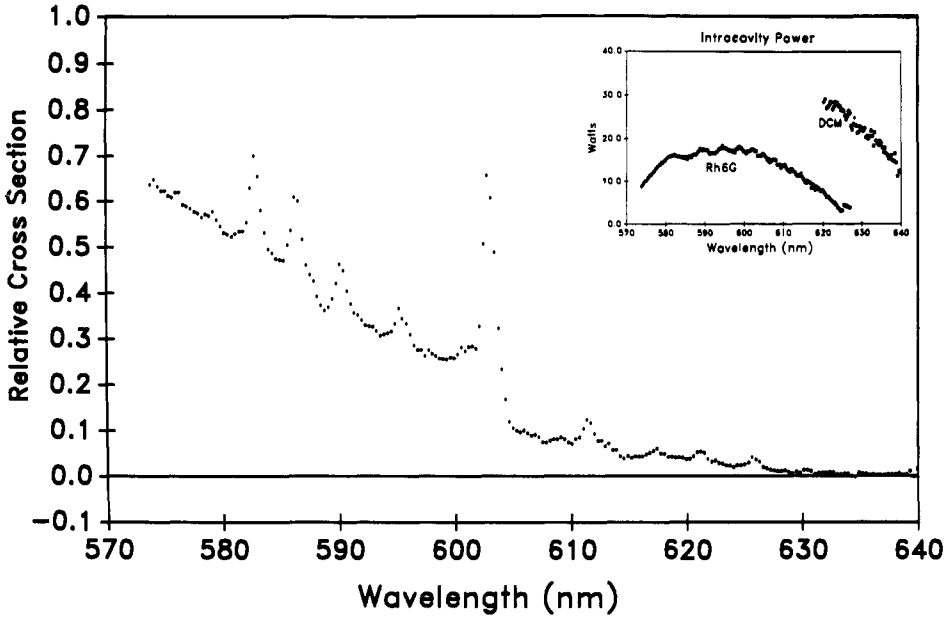

Figure 2. Experimental EPD cross section vs wavelength plot for the acetophenone enolate anion. The spacing between data points is ~3 Å.

constant describing the overlap between the photons and that portion of the ion swarm subtended by the detection system, are undetermined constants in these experiments and are omitted in calculating σ_{rel}.

The noise level in these experiments was determined by operating the FA with and without the laser system on and comparing the values of I and I_0. In the three studies reported here, the ion signals were $>10^5$ counts/s and the noise was <0.5% of this value. Data acquisition at wavelengths where >5% EPD was observed involved, at least, three separate samples of up to 200 laser-on/laser-off cycles. However, for wavelengths where <5% EPD was observed (especially in determination of the EPD threshold) or where other structural features were believed to occur, larger numbers of counting cycles (~1000) were taken to reduce the uncertainty.

Multiple measurements of the EPD spectral segments with a particular dye for the three negative ions reported herein demonstrated the reproducibility of the thresholds and other features, if present, to ±3 nm. This includes the ±1-nm uncertainty in measuring the starting and final wavelengths of the runs with the monochromator.

To establish the EPD as a one-photon process, the percentage of EPD $((I_0 - I)/I_0)$ at a particular wavelength was determined as a function of the intracavity photon power (output voltage of the power meter). The linear relationship with unit slope obtained from the ln–ln plot of these two functions ruled out any higher order process.

One problem in these experiments is the folding together of σ_{rel} vs λ plots obtained from two or more dyes where σ_{rel} (percent EPD) is large; this problem is absent in the threshold region where the percent EPD is small. When changing from one dye to another, the optics within the dye laser and the high reflective mirror must also be changed. These changes in the optics require a realignment and adjustments of the extended cavity to achieve maximum power and the best mode for EPD. This can produce small offsets of the σ_{rel} vs λ plots for the two dyes most likely caused by a small difference in the somewhat eliptical on-axis diameter of the photon beam through which the ions pass.[21] These offsets were removed by scaling the separate plots to give continuity. If a structural feature in the plot is evident at or near this union point, the normalization will be made at several different wavelengths; the useful wavelength ranges of the dyes employed overlap by ≥10 nm. This allows us to determine if the feature is valid or an artifact of the scaled union.

In our FA design, the first sampling molybdenum nose cone and its larger aluminum holder are electrically isolated from each other and from the ground of the flow reactor and electronics. Separate potentials are applied to the nose cone and its holder to optimize the negative ion signal intensity. We have observed that the percent EPD is markedly augmented by increasing the applied potential to the nose cone and halving the potential applied to the holder. While this operation leads to a decrease in the ion signal intensity (~25%), the increase in percent EPD by 200–300% makes its use desirable, especially in the threshold regions. We have observed no change in the envelope of the photodetachment spectrum of acetophenone enolate anion or in the EPD thresholds for c-$C_5H_5^-$ and c-$C_5H_4^{\bullet-}$ within the error limits using this procedure. The reason for this advantageous change in the percent EPD as a function of nose cone and holder potentials may be due to a change in the ion sampling under the two conditions, with a larger fraction of the sampled ions passing through the photon beam with the altered potentials.

Results and Discussion

I. Electron Photodetachment of Acetophenone Enolate Anion. In a series of EPD studies of aldehyde and ketone enolate anions, Brauman et al.[22] reported the photodetachment of acetophenone enolate anion in their ion cyclotron resonance spectrometer. The presence of several structural features in the σ_{rel} vs λ plot prompted us to reexamine this negative ion as a "test" of our apparatus and method. The plot is shown in Figure 2, with the insert showing the intracavity powers per wavelength for the two dyes employed, Rh6G and DCM. The agreement between the present plot in Figure 2 and the previous report is excellent. We were able to observe an additional weak feature at 627 nm by switching to DCM as the dye with its attendent increase in power at the longer wavelengths.

Not only was good Franck–Condon overlap for the negative ion and the radical required to observe such structure, the researchers suggested[7,22] that a bound dipole-supported electronic state of the anion existed, lying just below the threshold energy. In this diffuse electronic state, the electron is bound by the dipole of the radical with μ_{min} = 1.625 D. Brauman et al.[22] assigned the large sharp peak centered at 602.6 nm as the 0–0 transition. Extrapolation of the low-energy slope of this peak to $\sigma_{rel} = 0$ gives the onset at 606 nm and corresponds to the adiabatic EA of the $C_6H_5C(=O)CH_2^{\bullet}$ radical. The peaks superimposed on the increasing EPD continuum at higher energy than the 0–0 transition were assigned to a vibrational progression of the dipole-supported state of the radical and the electron. The weaker peaks observed at energies lower than the 0–0 transition are likely due to transitions from vibrationally excited negative ions in the 298 K manifold of this large enolate structure to the dipole-supported state, i.e., hot bands.[23] The ability of both Brauman's and our laser systems to resolve vibrational structure is clearly established by these results.

To demonstrate that the principal photodestruction process of acetophenone enolate anion was EPD, SF_6, which has a large electron attachment cross section, was added to the flow containing the negative ion. With the laser off, no change was observed.

(22) (a) Zimmerman, A. H.; Brauman, J. I. *J. Chem. Phys.* **1977**, *66*, 5823. (b) Jackson, R. J.; Zimmerman, A. H.; Brauman, J. I. *J. Chem. Phys.* **1979**, *71*, 2088.

(23) In the absence of the observed transitions, assignment of the low-energy EPD onset at 629 nm due to the hot bands rather than the 606-nm onset for the 0–0 transition would have underestimated EA($C_6H_5C(=O)CH_2^{\bullet}$) by 1.7 kcal mol^{-1}.

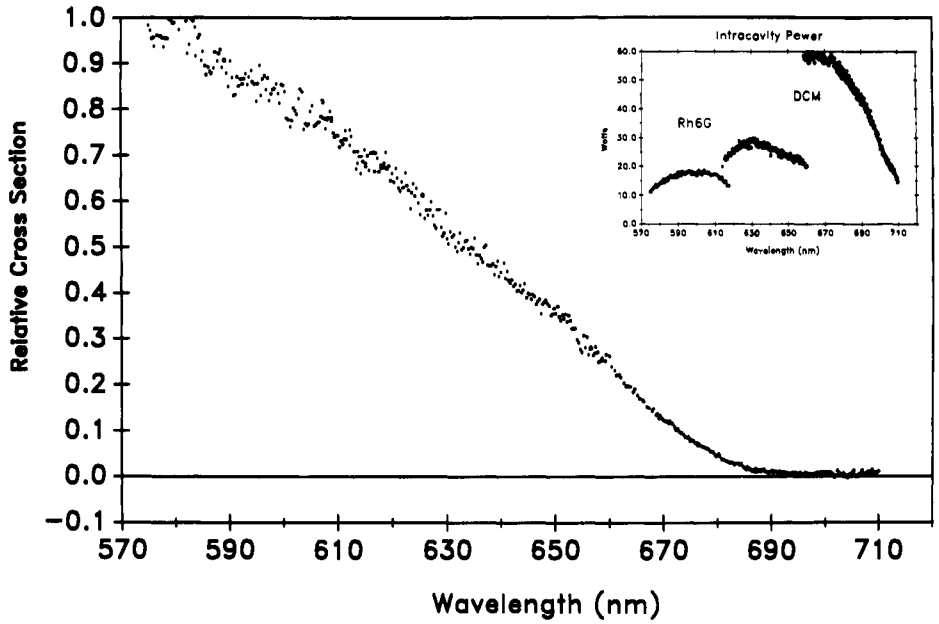

Figure 3. Experimental EPD cross section vs wavelength plot for the cyclopentadienyl anion. The spacing between data points is ~2 Å.

Table I. Summary of the Experimental and Calculated $\Delta H_f°$ of the Ground State and Certain Excited Electronic States of Cyclopentadienylidene (c-C_5H_4)

electronic state of c-C_5H_4	obsd threshold,[a] nm (kcal mol^{-1})	exptl $\delta\Delta H_f°$,[a] kcal mol^{-1}	calcd $\delta\Delta H_f°$, kcal mol^{-1}		$\Delta H_{f,298}$ of the state,[a,d] kcal mol^{-1}
			BBFOSV[b]	CDS[c]	
$^3B_1$	708 (40.4 ± 1.08)[e]	0.0	0.0	0.0	112.3 ± 4.7
$^1A_2$	619 (46.2 ± 0.23)[e]	5.8 ± 1.3	7.3	6.3	118.1 ± 4.7
$^3A_2$	598 (47.8 ± 0.23)[e]	7.4 ± 1.3	8.4	6.8	119.7 ± 4.7
[$^1A'$	576 (49.6 ± 0.23)[e]	9.2 ± 1.3	12.2		121.5 ± 4.7][f]

[a] This study. [b] Reference 39. [c] Reference 40. [d] Based on $\Delta H_{f,298}^{\circ}$(c-$C_5H_4^{\bullet-}$) = 71.9 ± 3.6 kcal mol^{-1}; see text and ref 42. [e] The rotational correction is only applied to the 708-nm threshold. For the excited-state transitions, the rotational onset will be part of the EPD background preceding the plateau. [f] Tentative assignment.

However, with the laser on, a SF_6^- ion signal was observed that accounted for ~50% of the loss in the signal intensity for the enolate anions.

II. Electron Photodetachment of Cyclopentadienyl Anion. The next problem was to determine the accuracy of the EPD threshold measurements for anions incapable of yielding a dipole-supported state. The cyclopentadienyl anion (c-$C_5H_5^-$) with its D_{5h} symmetry and relationship to c-$C_5H_4^{\bullet-}$ was selected for this purpose. Richardson et al.[24] had reproted the σ_{rel} vs photon energy plot for EPD of c-$C_5H_5^-$ over the energy range of 4.59–1.85 eV, and Engelking and Lineberger[25] determined EA(c-$C_5H_5^{\bullet}$) = 1.786 ± 0.020 eV by PES.

The EPD plot of σ_{rel} vs λ is shown in Figure 3 with the power curves of the two dyes used, Rh6G and DCM. As the threshold was approached, the intracavity power using DCM was increased in the range of ~655–710 nm by increasing the pumping power of the argon ion laser. The rise in the EPD σ_{rel} with increasing photon energy was similar to that reported in this energy range.[24]

The weak, unresolved hot bands observed in the PES spectrum of c-$C_5H_5^-$[25] are of the same order of magnitude as our noise level. The PES data were obtained with a low-pressure discharge ion source; this was prior to the use of an FA source by the Lineberger group.[26] Thus, the larger internal excitation of the sampled ions from the discharge source may lead to an increased hot band intensity compared to rotationally and vibrationally relaxed ions in the FA used here. We conclude that hot bands do not contribute to the present EPD threshold. The rotational corrections ($1.5kT$) of 0.045 eV are included in the error bars for these determinations.

On the basis of these considerations, the observed threshold at 693 ± 3 nm yields an electron affinity of 1.789 ± 0.047 eV for c-$C_5H_5^-$ in excellent agreement with the value determined by PES.[25]

If the data points for the region of 670–700 nm were fitted by the threshold law,[27] a value for the threshold of 697 nm (1.779 eV) is obtained. The σ_{rel} near the threshold is proportional to $(E - E_0)^{3/2}$ where E is the photon energy and E_0 is the threshold energy.[24]

Engelking and Lineberger[25] observed weak peaks in the photoelectron spectrum at 900 ± 100 and 3300 ± 100 cm^{-1} and assigned them as a symmetric C–H stretch and the symmetric ring breathing mode, respectively. Only the C–H stretch would be within the range of energies used here. However, no structural feature was observed on fitting the data to a cubic spline function and taking the first derivative.[28,29]

III. Electron Photodetachment of Cyclopentadienylidene Anion Radical. The target of this investigation was to determine the EPD threshold for cyclopentadienylidene anion radical (c-$C_5H_4^{\bullet-}$) to obtain the EA of the carbene cyclopentadienylidene (c-C_5H_4). The ground state of the carbene was observed to be a triplet ($^3B_1$) on the basis of the ESR spectra obtained at low temperatures in solid media.[30,31] EHT MO calculations[32] agreed with this as-

(24) Richardson, J. H.; Stephenson, L. M.; Brauman, J. I. *J. Chem. Phys.* **1973**, *59*, 5068.
(25) Engelking, P. C.; Lineberger, W. C. *J. Chem. Phys.* **1977**, *67*, 1412.
(26) Leopold, D. G.; Murray, K. K.; Miller, A. E. S.; Lineberger, W. C. *J. Chem. Phys.* **1985**, *83*, 4849.
(27) (a) Wigner, E. P. *Phys. Rev.* **1948**, *73*, 1002. (b) Geltman, S. *Phys. Rev.* **1958**, *112*, 176. (c) Burch, D. S.; Smith, S. J.; Branscomb, L. M. *Phys. Rev.* **1958**, *112*, 171. (d) O'Malley, T. F. *Phys. Rev.* **1965**, *137*, 1668. (e) Reed, K. J.; Zimmerman, A. H.; Andersen, H. C.; Brauman, J. I. *J. Chem. Phys.* **1976**, *64*, 1368. (f) Engelking, P. C. *Phys. Rev. A* **1982**, *26*, 740. (g) Schultz, P. A.; Mead, R. D.; Jones, P. L.; Lineberger, W. C. *J. Chem. Phys.* **1982**, *77*, 1153.
(28) (a) Proctor, A.; Sherwood, P. M. A. *Anal. Chem.* **1982**, *54*, 13. (b) *Ibid.* **1980**, *52*, 2315.
(29) This method of resolving structure in EPD spectra was reported by Janousek, B. K.; Zimmerman, A. H.; Reed, K. J.; Brauman, J. L. *J. Am. Chem. Soc.* **1978**, *100*, 6142.

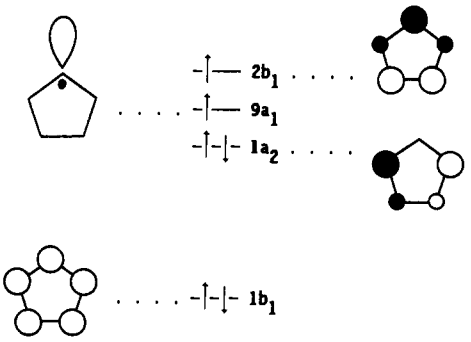

Figure 4. Qualitative molecular orbital diagram for the four highest occupied orbitals for the $^3B_1$ ground state of cyclopentadienylidene.

signment in that the in-plane σ ($9a_1$) orbital at C_1 and the delocalized π ($2b_1$) MO are close in energy.

Several other theoretical studies[33-40] of the carbene have been reported. Kassaee et al.[38] found that the C_{2v} structures for the singlet states $\mathbf{1}(\sigma^2)$and $\mathbf{2}(\pi^2)$ are not true potential energy minima using MNDO. The single imaginary vibrational frequency calculated for C_{2v} $\mathbf{1}(\sigma^2)$ distorts the C_{2v} geometry into the nonplanar C_s structures **3** ($^1A'$). Similarly, the two imaginary vibrational frequencies found for $\mathbf{2}(\pi^2)$ transform the structure into a twisted allenic C_s structure (**4**). Bofill et al.[39] using MNDO and ab initio

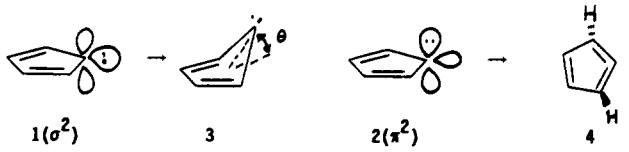

calculations also considered possible open-shell singlet states and calculated structures and total energies of the $^3B_1$ ground state and nine excited states of the carbene. Of the excited states, only the $^3A_2$, $^1A_2$, and $^1A'$ could be observed in the present experiments due to the laser wavelengths available. The calculated $\delta\Delta H_f°$ for these three excited states relative to the $^3B_1$ ground state are given in the fourth column of Table I. Most recently, Collins et al.[40] reported the results of higher level ab initio calculations of the ground and first two excited states of c-C_5H_4. These latter researchers concluded that the excited $^1A_2$ and $^3A_2$ states were "degenerate within the accuracy of the present theoretical methods, but more complete treatment of the correlation problem should favor the singlet". The $\delta\Delta H_f°$ calculated for these three states at the CISD(TZ2P, DZP)+Q level are listed in the fifth column of Table I.

The qualitative energies for the four highest energy bonding molecular orbitals of the triplet ground state of c-C_5H_4 are shown in Figure 4 with the appropriate drawings of the major atomic orbital contributions to these molecular orbitals.[39,40] The $^3B_1$ ground state has the partial electronic configuration $(1b_1)^2(1a_2)^2(9a_1)^1(2b_1)^1$ while the first two excited states predicted by theory are the $^1A_2$ and $^3A_2$ states with the partial electronic configuration $(1b_1)^2(1a_2)^1(9a_1)^1(2b_1)^2$. The third excited state of c-C_5H_4 is a $^1A'$ state that corresponds to Walli's nonplanar structure **3** with $\theta = 22.8°$.[39] From these calculations, the partial electronic configuration of the ground-state doublet carbene anion radical c-$C_5H_4^{\cdot-}$ should be $(1b_1)^2(1a_2)^2(9a_1)^2(2b_1)^1$, a $\sigma^2\pi^1$ species.

The pertinent background information on the carbene anion radical is that it is readily generated from diazocyclopentadiene[41] according to eq 5.[16b] c-$C_5H_4^{\cdot-}$ (m/z 64) undergoes facile coupling with the diazo compound precursor to yield the product ions at m/z 148 and 120 shown in eq 7 in a 3/1 ratio. The $\Delta H_{f,298}°$(c-

$$\underset{m/z\ 64}{\text{c-}C_5H_4^{\cdot-}} + \text{c-}C_5H_4N_2 \xrightarrow{\text{He}} \underset{m/z\ 148}{\text{(c-}C_5H_4)=NN=\text{(c-}C_5H_4)^{\cdot-}} \quad (7a)$$

$$\rightarrow \underset{m/z\ 120}{\text{(c-}C_5H_4)=\text{(c-}C_5H_4)^{\cdot-}} + N_2 \quad (7b)$$

$C_5H_4^{\cdot-}$) = 70.7 ± 3.2 kcal mol^{-1} [16b] (using $\Delta H_{f,298}°(H^+)$ = 367.2 kcal mol^{-1})[42] was determined; this value is now adjusted to 71.9 ± 3.6 kcal mol^{-1} on the basis of corrected values for the proton affinities of the alcohols used to bracket PA(c-$C_5H_4^{\cdot-}$).[42]

In the initial EPD experiments using Rh6G as the dye, an *increase* rather than a decrease in the ion signal at m/z 64 was observed particularly at the longer wavelengths in the laser-on periods. This increase was found to be approximately equal to the amount of the secondary product azine anion radical ions at m/z 148 (eq 7a) present in the flow and photodecomposed at these wavelengths. Apparently, the ions at m/z 148 photodissociate, at least partially, to yield c-$C_5H_4^{\cdot-}$ and c-$C_5H_4N_2$ (or c-C_5H_4 + N_2). This problem is eliminated by significantly reducing the concentration of the precursor diazo compound present in the flow. Careful addition of a dilute gas mixture of c-$C_5H_4N_2$ (1–2%) in helium to just remove all electrons at a point halfway down the length of the flow tube produced only a trace of the signal for the m/z 148 ions.

Under the above conditions, the σ_{rel} vs λ EPD plot shown in Figure 5a was determined. The three dyes involved in this plot were Rh110, Rh6G, and DCM. The assignment of the threshold is 708 ± 3 nm (arrow at right of plot). Fitting of the data from 680 to 720 nm with the threshold law[27] gave a threshold of 715 nm, in good agreement with the above value.

Inspection of Figure 5a showed the likelihood of two breaks in the EPD σ_{rel} vs λ plot at about 620 and 600 nm. These two features are more clearly distinguished when the first (Figure 5b) and second derivatives were obtained on the smoothed data. The "plateau" centers were found to be at 619 ± 3 and 598 ± 3 nm. The derivative curves also suggested that a third plateau may be present at 576 ± 3 nm, although this feature is not as sharply defined and must be considered tentative.

The threshold corresponding to the lowest energy for the EPD process is the EA of the ground state of the carbene c-C_5H_4. The measured threshold at 708 ± 3 nm for c-$C_5H_4^{\cdot-}$ is nearly the same as that of the corresponding carbanion c-$C_5H_5^-$ (693 ± 3 nm). This similarity of threshold values between the carbene anion radical ($R_2C^{\cdot-}$) and the corresponding carbanion (R_2CH^-) has recently been observed in the related pairs (indenylidene anion radical)–(indenyl anion) and (fluorenylidene anion radical)–(fluorenyl anion).[46] The energy spacings between the threshold

(30) Wasserman, E.; Barash, L.; Trozzolo, J.; Murray, R. W.; Yager, W. A. *J. Am. Chem. Soc.* **1964**, *86*, 2304.
(31) For the UV and IR spectra of the matrix isolated carbene, see: Baird, M. S.; Dunkin, I. R.; Hacker, N.; Poliakoff, M.; Turner, J. J. *J. Am. Chem. Soc.* **1981**, *103*, 5190.
(32) Gleiter, R.; Hoffman, R. *J. Am. Chem. Soc.* **1968**, *90*, 5457.
(33) Lee, C. K.; Li, W. K. *J. Mol. Struct.* **1977**, *38*, 253.
(34) Shepard, R.; Simons, J. *Int. J. Quantum Chem.* **1980**, *S14*, 349.
(35) Kausch, M.; Curr, H. *J. Chem. Res., Synop.* **1982**, 2.
(36) Tsang, H. T.; Li, W. K. *Croat. Chem. Acta* **1983**, *56*, 103.
(37) Glidewell, C.; Lloyd, D. *J. Chem. Res., Synop.* **1983**, 178.
(38) Kassee, M. Z.; Nimlos, M. R.; Downie, K. E.; Waali, E. E. *Tetrahedron* **1985**, *41*, 1579.
(39) Bofill, J. M.; Bru, N.; Farras, J.; Olivella, S.; Sole, A.; Villarrasa, J. *J. Am. Chem. Soc.* **1988**, *110*, 3740.
(40) Collins, C. L.; Davy, R. D.; Schaefer, H. F. *Chem. Phys. Lett.* **1990**, *171*, 259.
(41) Doering, W. von E.; DePuy, C. H. *J. Am. Chem. Soc.* **1953**, *75*, 5955.
(42) PA(c-$C_5H_4^{\cdot-}$) = 377.0 ± 2.0 kcal mol^{-1} was determined by extrapolation of the plot of the percent proton transfer vs the $\Delta H°_{acid}$ of the three alcohols C_2H_5OH, *n*-C_3H_7OH, and *t*-C_4H_9OH used in the bracketing.[16b] The new value for PA(C_2H_5OH) = 377.3 ± 2.4 kcal mol^{-1} [43] leads to PA(c-$C_5H_4^{\cdot-}$) = 378.2 ± 2.4 kcal mol^{-1}. From this value, $\Delta H_{f,298}°$(c-$C_5H_5^{\cdot}$) = 60.9 ± 1.2 kcal mol^{-1},[44] and $\Delta H_{f,298}°(H^+)$ = 367.2 kcal mol^{-1},[45] $\Delta H_{f,298}°$(c-$C_5H_4^{\cdot-}$) = 71.9 ± 3.6 kcal mol^{-1} is calculated. These values differ from those given in a recent standard reference[43] partly due to the different convention for H^+ and a 1 kcal mol^{-1} difference in assigning the PA(c-$C_5H_4^{\cdot-}$).
(43) Lias, S. G.; Bartmess, J. E.; Liebman, J. F.; Holmes, J. L.; Levin, R. D.; Mallard, W. G. *J. Phys. Chem Ref. Data, Suppl.* **1988**, *17*.
(44) Furuyama, S.; Golden, D. M.; Benson, S. W. *Int. J. Chem. Kinet.* **1971**, *3*, 237.
(45) Stull, D. R., Prophet, H., Eds. JANAf Thermochemical Tables. *Natl. Stand. Ref. Data Ser., Natl. Bur. Stand.* **1971**, *No. 37*.
(46) McDonald, R. N.; Tung, C. C. Unpublished results.

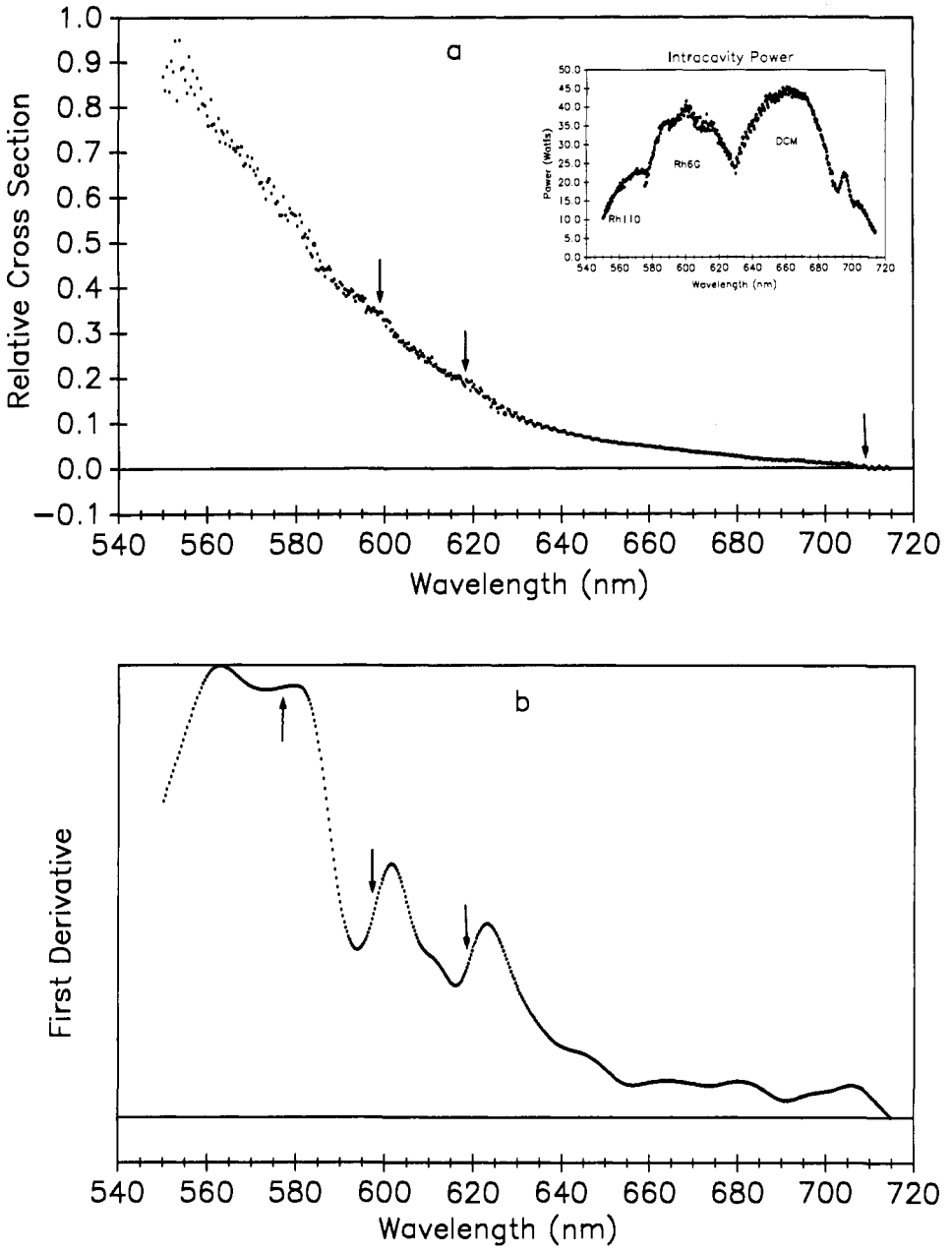

Figure 5. (a) Experimental EPD cross section vs wavelength plot for the cyclopentadienylidene anion radical. The spacing between data points is ~2 Å. (b) First derivative of the smoothed data in Figure 5a.

(708 nm) and the two features at 619 and 598 nm are fortuitously similar to those reported for EPD of phenylnitrene anion radical ($PhN^{\bullet -}$).[47]

The experiments in the FA are carried out in a large, fast flow of helium buffer gas for collisional thermalization of the negative ions. If hot band transitions were to occur, a series of closely spaced transitions would be expected from population of other high- and low-frequency modes in the carbene anion radical, as was observed for the weak transitions at longer wavelengths than the 0–0 transition for the acetophenone enolate anion. This and the large energy gap between the first (708 nm) and second transitions (619 nm) eliminates the possibility that the first or second onsets are due to hot band transitions from excited vibrational levels of the anion to lower levels of the carbene.

Our inability to observe the weak hot bands in the EPD of the carbanion $c\text{-}C_5H_5^-$ described in the previous section strongly suggests that this will be the case in the present experiments. Therefore, we conclude that hot bands make no significant contribution to the observed cross section at the 708-nm threshold observed in Figure 5a for the closely related $c\text{-}C_5H_4^{\bullet -}$ species. However, the same correction for the rotational onset is incorporated into the assigned error limit of ±0.047 eV to the threshold at 708 nm.

The results of the two theoretical papers involving ab initio calculations of $c\text{-}C_5H_4$[39,40] suggest that the thresholds yielding the first three excited states of the carbene are within the energy range examined in this study. The values of the threshold and plateaus observed for the EPD of $c\text{-}C_5H_4^{\bullet -}$ are listed in the second column of Table I. The energy differences between the plateaus and that of the threshold are given in column three. The good agreement between the experimental and calculated energy differences given in columns four and five suggest that these are the transitions observed in the present study. However, we note that the existence of a transition at 576 ± 3 nm is tentative. The $\Delta H^\circ_{f,298}$ of the carbene electronic states are calculated by adding the EPD threshold values (kcal mol^{-1}) to $\Delta H^\circ_{f,298}(c\text{-}C_5H_4^{\bullet -})$ in Table I.

From these and certain other data, we can estimate the bond dissociation energy of the C–H bond in the cyclopentadienyl radical from a thermochemical cycle leading to eq 8; $PA(c\text{-}C_5H_4^{\bullet -})$

$$D^\circ(c\text{-}C_5H_4\text{–}H) = PA(c\text{-}C_5H_4^{\bullet -}) + EA(c\text{-}C_5H_4) - IP(H) \quad (8)$$

(47) Drzaic, P. S.; Brauman, J. I. *J. Am. Chem. Soc.* **1984**, *106*, 3443.

= 378.2 ± 2.4 kcal mol^{-1}.[42] From this approach, $D°(c\text{-}C_5H_4\text{-}H)$ = 105.0 ± 3.4 kcal mol^{-1}, which is the same value as that calculated for the carbanion, $D°(c\text{-}C_5H_4^-\text{-}H)$ = 104.2 ± 7 kcal mol^{-1}.[48] Thus, the presence of five or six π-electrons does not influence the C-H bond strengths in these two molecules.

Conclusions

A flowing afterglow coupled with a CW laser system has been developed for the accurate determination of electron affinities of neutral molecules from threshold measurements of EPD of the corresponding negative ions. With this apparatus, the EPD thresholds of the doublet ground state of cyclopentadienylidene anion radical, $c\text{-}C_5H_4^{\bullet-}$, yielding the ground ($^3B_1$ at 708 nm) and certain excited states ($^1A_2$ at 619 nm, $^3A_2$ at 598 nm, and, tentatively, $^1A'$ at 576 nm) of the corresponding carbene have been measured. From these data and the previously determined $\Delta H°_{f,298}(c\text{-}C_5H_4^{\bullet-})$, the $\Delta H°_{f,298}(c\text{-}C_5H_4)$ for the ground and excited states are calculated. It is further shown that the C-H bond dissociation energies in $c\text{-}C_5H_5^{\bullet}$ and $c\text{-}C_5H_5^-$ are the same within the broad error limits.

Acknowledgment. We thank the National Science Foundation for support of this research and Professor D. W. Setser for a number of suggestions and helpful discussions. We also thank Mr. John Linzi for design and construction of the circuit that allowed for recovery of the eight digits of data from the photon counter/processor.

Registry No. $C_6H_5C(=O)CH_2^{\bullet}$, 50781-28-7; $c\text{-}C_5H_5^-$, 12127-83-2; $c\text{-}C_5H_5^{\bullet}$, 2143-53-5; $c\text{-}C_5H_4^{\bullet-}$, 75137-28-9; $c\text{-}C_5H_4$, 4729-01-5; acetophenone enolate anion, 34438-71-6.

(48) $\Delta H°_{f,298}(c\text{-}C_5H_5^-)$ = 19.6 ± 3.8 kcal mol^{-1}.[43]

Electronic Excitation in Low-Energy Collisions: A Study of the Collision-Induced Dissociation of Nitromethane Ion by Crossed-Beam Tandem Mass Spectrometry

Kuangnan Qian, Anil Shukla, and Jean Futrell*

Contribution from the Department of Chemistry and Biochemistry, University of Delaware, Newark, Delaware 19716. *Received December 14, 1990*

Abstract: The dynamics of collision-induced dissociation (CID) of nitromethane ion have been investigated with an angle-resolved crossed-beam tandem mass spectrometer. Kinetic energy and angular distributions of two main products of the dissociation, NO^+ and NO_2^+, were measured at center-of-mass (CM) collision energies from 1.5 to 119 eV. Impulsive mechanisms are involved for NO_2^+ formation at all energies investigated. At and below 3-eV collision energy, a rebound reaction mechanism is observed, implying small impact parameter collisions dominate the CID process. A transition from backward to forward scattering is observed for NO_2^+ in the collision energy range of 3–6 eV. At higher energies, NO_2^+ formation is progressively more forward scattered but never approaches zero scattering angle within the energy range studied. The mechanism for forming NO^+ is uniquely different from NO_2^+ in that two intensity maxima are observed at all energies, suggesting that the dissociation proceeds via at least two reaction pathways. The peak maximum at 0° is attributed to dissociation following isomerization of nitromethane ion to methyl nitrite ion while the back-scattered peak follows an impulsive excitation reaction path similar to NO_2^+ formation and is attributed to nonisomerized nitromethane cations that require small impact parameter collisions to induce isomerization and dissociation. As the collision energy is increased, a highly endothermic dissociation process involving the transfer of 5.5–5.7-eV energy from translational to internal energy is also observed. Since the threshold for NO^+ formation is only 0.64 eV, it is suggested that these low-energy collisions lead to electronic excitation of nitromethane ion to the sixth ionization band of its photoelectron spectrum and that dissociation proceeds on the excited-state hypersurface.

Introduction

The unimolecular and collision-induced dissociation (CID) of the nitromethane ion and its isomer, methyl nitrite ion, have been extensively studied.[1-13] It has often been suggested[2,3,7] that their dissociation involves isolated electronic states and incomplete internal energy randomization in violation of the fundamental assumption of statistical theories—e.g., the Rice-Ramsperger-Kassel-Marcus (RRKM) theory of unimolecular reactions[14] and the quasi-equilibrium theory (QET) of mass spectra.[15] The present CID dynamics study was undertaken, in part, to search for reactive scattering features that might support this hypothesis. A preliminary account reporting such dynamics features has already been published.[16]

We have shown in previous publications that photoelectron spectra and experimentally determined breakdown graphs provide information useful for the interpretation of CID scattering experiments.[17] The photoelectron spectrum of nitromethane and its ionic breakdown graph measured by photoelectron-photoion coincidence (PEPICO) technique are shown in Figure 1. The thermochemically predicted onsets and experimentally measured dissociation energies for different dissociation processes are listed in Table I. The breakdown graph for the nitromethane ion shows[2] that the formation of NO^+ proceeds via at least two different

(1) Lifshitz, C.; Rejwan, M.; Levin, I.; Peres, T. *Int. J. Mass Spectrom. Ion Processes* **1988**, *84*, 271.
(2) Niwa, Y.; Tajima, S.; Tsuchinya, T. *Int. J. Mass Spectrom. Ion Phys.* **1981**, *40*, 287.
(3) Ogden, I. K.; Shaw, N.; Danby, C. J.; Powis, I. *Int. J. Mass Spectrom. Ion Phys.* **1983**, *54*, 41.
(4) Egsgaard, H.; Carlsen, L.; Elbel, S. *Ber. Bunsen-Ges. Phys. Chem.* **1986**, *90*, 369.
(5) Baer, T.; Hass, J. R. *J. Phys. Chem.* **1986**, *90*, 451.
(6) Ferguson, E. E. *Chem. Phys. Lett.* **1987**, *138*, 450.
(7) Gilman, J. P.; Hsieh, T.; Meisels, G. G. *J. Chem. Phys.* **1983**, *78*, 1174.
(8) (a) Meisels, G. G.; Hsieh, T.; Gilman, J. P. *J. Chem. Phys.* **1980**, *73*, 4126. (b) Gilman, J. P.; Hsieh, T.; Meisels, G. G. *J. Chem. Phys.* **1983**, *78*, 3767.
(9) Sirois, M.; Holmes, J. L.; Hop, C. E. C. A. *Org. Mass Spectrom.* **1990**, *25*, 167.
(10) Todd, P. J.; Warmack, R. J.; McBay, E. H. *Int. J. Mass Spectrom. Ion Phys.* **1983**, *50*, 299.
(11) Zwinselman, J. H.; Nacson, S.; Harrison, A. G. *Int. J. Mass Spectrom. Ion Processes* **1985**, *67*, 93.
(12) Hubick, A. R.; Hemberger, P. H.; Laramee, J. A.; Cooks, R. G. *J. Am. Chem. Soc.* **1980**, *102*, 3997.
(13) McKee, M. L. *J. Phys. Chem.* **1986**, *90*, 2335.
(14) Marcus, R. A.; Rice, O. K. *J. Phys. Colloid Chem.* **1951**, *55*, 894.
(15) Rosenstock, H. M.; Wallenstein, M. B.; Wahrhaftig, A. L.; Eyring, H. *Proc. Natl. Acad. Sci. U.S.A.* **1952**, *38*, 667.
(16) Qian, K.; Shukla, A.; Futrell, J. *Rapid Commun. Mass Spectrom.* **1990**, *4*, 222.
(17) Qian, K.; Shukla, A.; Futrell, J. *J. Chem. Phys.* **1990**, *92*, 5988.

0002-7863/91/1513-7121$02.50/0